



Received Date : 29-Mar-2019  
Revised Date : 25-Apr-2019  
Accepted Date : 01-May-2019

Article type : Research Letter

Overexpression of the dopamine receptor-interacting protein Alix/AIP1 modulates NMDA receptor-triggered cell death

Sharifah Salim<sup>1</sup>, Jamal Nasir<sup>2</sup> and Philip E Chen<sup>1#</sup>

<sup>1</sup>  
Centres for Biomedical Sciences and Gene & Cell Therapy, School of Biological Sciences,  
Royal Holloway, University of London, Egham, Surrey, UK

<sup>2</sup>  
Molecular Biosciences Research Group, Faculty of Health & Society, University of  
Northampton, Waterside Campus, Northampton, UK

#Address correspondence to Philip Chen,

Centres for Biomedical Sciences and Gene & Cell Therapy, School of Biological Sciences,  
Royal Holloway, University of London, Egham, Surrey, UK

Tel: +44-1784 44 3386

Email: philip.chen@rhul.ac.uk

Running title: Alix influences NMDA receptor-triggered cell death

This article has been accepted for publication and undergone full peer review but has not been through the copyediting, typesetting, pagination and proofreading process, which may lead to differences between this version and the Version of Record. Please cite this article as doi: 10.1002/1873-3468.13434

## **Abstract**

Alix/AIP1 is an adaptor protein involved in apoptosis, endocytic membrane trafficking and brain development. Alix has been found within the human postsynaptic density (PSD) and, since NMDA receptors (NMDARs) are central components of the PSD, we hypothesized that the close proximity of both proteins may allow Alix to influence the downstream pathways following NMDAR activation. NMDARs play important roles in excitotoxicity, and we evaluated the effects of recombinant Alix in an NMDAR cell death assay. Overexpression of Alix with NMDARs increases the potency of NMDAR-induced cell death compared to cells expressing only NMDARs, and this requires expression of the Alix C-terminal region. Therefore, we demonstrate a previously unreported role for Alix as a potential modulator of NMDAR function.

**Key words:** ALG-2, Alix/AIP1, calcium, dopamine receptor interacting protein, excitotoxicity, glutamate receptor, neurodegeneration, PDCD6IP, postsynaptic density

## **Abbreviations**

ALG-2, apoptosis-linked gene 2, AIP1, ALG-2 interacting Protein 1, APV, 2*R*-amino-5phosphonopentanoate, PSS, Physiological Salt Solution, NMDA, N-methyl-D-aspartate

## **Introduction**

Glutamate-induced neuronal cell death via NMDAR excitotoxicity is thought to contribute to many neurodegenerative processes within the mammalian CNS [1]. The influx of Ca<sup>2+</sup>

This article is protected by copyright. All rights reserved.

through NMDARs is vital for cell death to occur and is important for stimulating a variety of intracellular signaling cascades although the precise molecular mechanisms of  $Ca^{2+}$  dependent cytotoxicity still remain unclear [2]. The roles of NMDARs in neuronal death are complex and the synaptic or extrasynaptic location of NMDARs can influence the pathways leading to neuroprotection or neurotoxicity [3]. NMDARs are ligand-gated heteromeric ion channels composed of GluN1 and GluN2 subunits and the incorporation of the different GluN2 subunits (A-D) is a major determinant of both physiological and pathological NMDAR properties [4,5].

ALG-2 interacting protein (apoptosis-linked gene 2-interacting protein X /Alix/AIP1/PDCD6IP) is an ubiquitous adaptor protein that was first described for its capacity to bind to the calcium-binding protein, Apoptosis-linked gene-2 (ALG-2) [6,7]. It is known to be involved in apoptosis, regulation of cell adhesion, protein sorting, adaptation to stress conditions, ESCRT (endosomal sorting complex required for transport), brain development and neuronal cell death [8-13]. Furthermore, it has been identified as a novel dopamine receptor interacting protein, using D1 receptor C-terminal domain or D3 receptor third cytoplasmic loop as 'baits' in separate yeast two-hybrid screens [14]. Although there is clear evidence of Alix playing important roles in neuronal function [15,16], the precise purpose of Alix at the synapse requires further investigation. There is evidence that Alix may have a presynaptic role [9,17] but Alix has also been found within the human postsynaptic density (PSD) and is a CHMP4B binding protein within the PSD associated ESCRT-III complex [18,19]. Therefore, there is potential for Alix to facilitate intracellular 'cross talk' between neurotransmitter signalling pathways as well as modulate downstream signaling cascades following receptor stimulation. Given that dopamine receptors also interact with NMDARs [20,21], there is a well documented interaction between dopamine and glutamate signalling [22] and NMDARs are a central component of the PSD and have the capacity to

This article is protected by copyright. All rights reserved.

trigger  $\text{Ca}^{2+}$ -dependent neuronal cell death, we hypothesized that Alix may be able to influence NMDAR triggered cell death.

Using heterologous expression of recombinant proteins in HEK293 cells, we examined the effect of Alix coexpression on NMDAR-triggered cell death. Our results suggest that Alix is able to enhance NMDAR cell death in low or absent glutamate/glycine concentrations.

## Materials and Methods

*Plasmid cDNAs* cDNA plasmids for Alix (GFP tagged in pCMVTag2C) have been previously described [14].

Flag tagged mouse Alix (in pCI) and the Alix deletion mutants have been published [17]. The NMDAR subunit cDNAs GluN1 and GluN2A in pRK7 have been reported previously [23].

### *Cell culture and transient transfections of plasmid cDNAs*

HEK-293 cells were cultured in DMEM medium (Minimum Essential Medium,  $\alpha$  Modification [ $\alpha$ -MEM]) supplemented with 50 mg/ml Gentamycin, 4 mM L-glutamine, and 10 % fetal bovine serum). Cells were plated at a density of  $2 \times 10^5$  cells/1 ml DMEM medium onto each well of a 24 well tissue culture plate and incubated in a 5%  $\text{CO}_2$  incubator at 37 °C for 24 hours.

Cells were transiently transfected using lipofectamine 2000 (Invitrogen). The DNA plasmid / lipofectamine mix and 100  $\mu\text{l}$  of DMEM medium (without FBS, L-glutamine and antibiotics) were added to each well of a 24 well plate with 1 ml of medium containing

This article is protected by copyright. All rights reserved.

attached cells at approximately 50-85% confluency. Cells were left for 18- 20 hours at 37 °C in a 5% CO<sub>2</sub> incubator. In experiments that used two, three or four different plasmids, equal concentrations of plasmids were added (total DNA concentration, 3 µg per well). To control for the effects of EGFP expression on cell death, pEGFP-N1 cDNA was added for GluN1/GluN2A only transfections. Transient transfections were performed with 10 µl lipofectamine/well. Using fluorescent cell counting, we observed maximal transfection efficiency of approximately 80 % for both GFP and GFP-tagged hAlix.

#### *Western blotting*

HEK-293 cells were grown to a density of  $1.2 \times 10^6$  cells and transiently transfected and treated as described above. Cells were trypsinised, spun down and washed twice with PBS. The pellet was then left in 2 ml 1/2x protease inhibitor (Roche) on ice for 1 hour, homogenised and then spun down at 16,000 rpm for 15 minutes. The pellet was solubilized with buffer Px to a 1:1 ratio (0.2 M sodium phosphate pH 7.5, 1 % Triton X-100 and supplemented with protease inhibitors) on ice for 1 hour. It was then spun down at 16,000 rpm for 2 minutes and the supernatant collected.

The concentration of the protein extract was determined by Bradford's Protein Assay. Protein samples were loaded on a 4-12 % pre-cast NuPage gel in XCell Sure Lock mini gel system (Invitrogen). The separated polypeptides were transferred to 0.45 µm nitrocellulose by electroblotting in 1 x transfer buffer (NuPage 20x transfer buffer, Invitrogen) using the Bio Rad mini system. The nitrocellulose paper was then blocked with blocking buffer (50 mM Tris Base, 150 mM NaCl, 0.1 % Tween-20 with 5 % milk) and aspirated immediately with SNAP i.d. (Merck Milipore) and washed three times with TBS-T (50 mM Tris Base, 150 mM NaCl, 0.1 % Tween 20). The blot was incubated with the mouse anti-Alix [3A9] antibody

(1:100 dilution, Abcam, ab117600) or mouse anti-GluN1 [54.1] (1:1000 dilution, BD Biosciences) overnight and then IRDye 800 goat anti-mouse (Licor) for 10 minutes and washed 3 times with TBS-T. The bound antibodies were visualized with the Odyssey Licor imaging system.

#### *Synaptosomal preparation*

This was based on a previously published protocol [24]. Adult rat cerebral cortex was removed, homogenized in cold isolation buffer (5 mM HEPES, 0.32 mM sucrose, pH 7.4) and centrifuged (1,500 g). The pellet was resuspended in 0.32 M sucrose, 1 mM NaHCO<sub>3</sub> and layered over a sucrose gradient (1.2/1/0.85 M) before centrifugation (70,000 g). The synaptosomal layer was harvested and resuspended in sodium resuspension media (2.5 mM HEPES, 8 mM KCl, 110 mM NaCl, 2.6 mM CaCl<sub>2</sub>, 10 mM glucose, pH 7.4).

#### *Primary cortical cultures*

E18 rat embryos were terminated under Schedule 1 Home Office procedures (UK). After removal of the skull, the brain was placed dorsal side up and noncortical tissue was removed. The remaining cortical tissue was placed in ice cold PBS and chopped into small pieces. The tissue was then incubated for 20 minutes in 1 ml of 25 % tryPLE/PBS solution at 37 °C before trituration in 37 °C DMEM. The solution was centrifuged at 1500 rpm and the cell pellet was resuspended in 1 ml Neurobasal medium supplemented with 2 % B27 serum free supplement, 1 % penicillin/streptomycin, 300 μM glutamine and 25 μM β-mercaptoethanol. The cells were plated at an approximate density of 2 x 10<sup>5</sup> per well of a 24-well plate. Neurones were maintained in culture for 14 days before use with fresh media added every 3-5 days.

#### *Immunofluorescence*

This article is protected by copyright. All rights reserved.

Transiently transfected HEK 293 cells were cultured at a density of  $1.75 \times 10^6$  cells in 24 well plates on glass cover slips coated with 100  $\mu\text{g/ml}$  poly-D-lysine. The cells were then fixed with 4 % Paraformaldehyde (PFA) for 10 min and washed three times with PBS on ice. Fixed cells were blocked with PBS containing 5 % horse serum and 0.1 % Tween-20 for 45 minutes at room temperature. The cells were then incubated with the appropriate primary (mouse anti-Alix, Abcam, 1:100 dilution, rabbit anti-PSD95, Abcam ab18258, 1:500 dilution mouse anti-EEA1, BD Biosciences, 610456, 1:1000 dilution) and secondary antibodies (Alexa Fluor 488 Goat anti-mouse secondary antibodies, Invitrogen, 1:1000 dilution) for 1 hour each before embedding. Nuclei were stained with Hoechst 33342 (Sigma) for 5 minutes at room temperature. F-actin was stained with TRITC-conjugated rhodamine-phalloidin (77481, Sigma) diluted in PBS for 30 minutes at room temperature. Following staining, cells were embedded using the ProLong Gold reagent (Invitrogen). The stained cells were visualised under a spinning disc confocal system (CARV from Digital Imaging Solutions) with an EM-CCD camera (Rolera/QI Cam 3500) mounted on an Olympus X71 microscope, using a 100 $\times$  plan objective. The microscope confocal system was supported by ImagePro 6.0 software. The same protocol was used to fix and stain primary cortical neurones after 14 days *in vitro*. The degree of colocalisation within a region of interest was performed using ImageJ. The colocalisation coefficients of each fluorophore pair were plotted as a scatter plot and a mean Pearson correlation coefficient was calculated to indicate the degree of colocalisation.

#### *NMDAR-triggered cell death assay*

The trypan blue exclusion assay to measure the extent of glutamate receptor triggered cell death has been described previously [25] [26] [27]. Cells were exposed to various treatments 18-20 hours after the start of the transfection. Control cells were incubated in a physiological salt solution (PSS; 140 mM, NaCl; 1.4 mM  $\text{CaCl}_2$ ; 5.4 mM KCl; 1.2 mM  $\text{NaH}_2\text{PO}_4$ ; 21 mM

glucose; 26 mM NaHCO<sub>3</sub>; pH 7.4) for 10 min in a 5% CO<sub>2</sub> incubator at 37 °C. Activation of NMDARs was performed by incubating the cells in PSS containing 1 mM NMDA (Tocris) and 50 μM glycine (Sigma) for 10 min. After the 10-min treatment, cells were placed in fresh media for six hours before assessment of cell death. 100 μM APV (Tocris) was added to each well to block any NMDAR activation before NMDA/glycine or PSS treatment.

Cell death was assessed by trypan blue exclusion after trypsinisation. This was determined by removing the PSS and media from each well and adding trypan blue (1:1 ratio). The number of stained cells and unstained cells were counted using a haemocytometer and calculated as a percentage of total cells. This was performed on cells attached to the well surface and on cells floating in the media or PSS. The percentage of stained or unstained cells from both attached and floating cells were combined to give a percentage cell death. All data points correspond to the mean ±SE of values performed from at least three separate transfections.

#### *Curve fitting and statistical analysis*

GraphPad Pro 6.12 (Wavemetrics) was used to fit dose-response curves of NMDAR triggered cell death with the Hill equation below:

$$I = I_{\max} / \{1 + (EC_{50} / [A])^{n_H}\}$$

$n_H$  is the Hill coefficient,  $I_{\max}$  is the maximum level of cell death,  $[A]$  is the concentration of agonist (NMDA) and  $EC_{50}$  is the concentration of agonist that produces a half-maximal response. Statistical comparisons of cell death between groups were performed using ANOVA followed by post-hoc Tukey's test to determine statistical significance.

## Results

In order to confirm efficient expression of the human N-terminal GFP tagged Alix protein in HEK293 cells (Figure 1A), we detected Alix expression using Western blotting and confocal microscopy (Figure 1). A distinct band was detected in protein extracts from Alix transfected cells but not untransfected cells (Figure 1B). In addition, we also examined NMDAR GluN1 subunit expression and detected no changes when coexpressed with Alix (Figure 1B). We also confirmed GFP-tagged Alix expression using confocal microscopy (Figure 1C-H). HEK293 cells transiently transfected with human GFP-tagged Alix displayed strong cytoplasmic expression in agreement with previous studies [7,14]. This localization was similar when Alix was transfected alone (Figure 1C-E) or coexpressed with NMDARs (Figure 1F-H). Furthermore, we also visualized GluN1 expression in cells coexpressed with Alix (Figure 1I-J). There is literature supporting Alix expression at postsynaptic locations [18,19], and we examined the expression of Alix in different subcellular extractions from rat brain (Figure 2A). We detected a distinct Alix band in the synaptosomal fraction compared to other fractions or adult brain homogenate which supports synaptic expression of this protein. Furthermore, we also examined endogenous Alix expression in rat primary cortical cultures.

Alix displayed punctate staining in the cytoplasm with little expression in the nucleus (Figure 2B-E). We examined whether this would be similar to proteins such as PSD-95 that are known to show postsynaptic localization. We observed a similar punctate expression in both Alix and PSD-95 stained cells (Figure 2F-I). Alix is involved in multivesicular body sorting and receptor trafficking [8,28] but this has not been observed in neurones. To investigate this, we examined the expression of the Early Endosome Antigen 1 (EEA1) which is a known marker for early endosomes. EEA1 staining showed a punctate pattern of expression and there was some overlap with Alix expression (Figure 2J-M). Colocalisation scatter analysis showed little correlation between Alix and Hoechst staining (mean Pearson correlation This article is protected by copyright. All rights reserved.

coefficient =  $-0.133 \pm 0.12$ ,  $n=3$ ) consistent with the cytoplasmic expression of Alix. However, we observed a more positive correlation between Alix and PSD95 ( $0.496 \pm 0.08$ ,  $n=3$ ) and Alix and EEA1 ( $0.406 \pm 0.07$ ,  $n=3$ ) staining. Therefore, Alix shows some expression at postsynaptic sites and endosomes which is consistent with previous reports.

We expressed GFP tagged human Alix together with GluN1 and GluN2A NMDAR subunits in HEK293 cells and examined NMDAR triggered cell death (Figure 3A and B). We found that cells expressing GluN1/GluN2A subunits treated with 1 mM NMDA/50  $\mu$ M glycine had a mean cell death of  $27.4 \pm 1.4$  % (Figure 3A). Whereas, cells expressing GluN1/GluN2A subunits and treated with physiological salt solution had a mean cell death of  $11.6 \pm 0.7$  % (Figure 3B). These results are similar to those reported by Wagey et al., 2001 [25] and confirmed expression of functional NMDARs. Coexpression of Alix with NMDARs and treating them with NMDA/glycine also produced a significant level of cell death but this was less than that seen with cells only expressing GluN1/GluN2A (mean cell death of  $21.6 \pm 1.9$  %, Figure 3A, ANOVA,  $p<0.01$ ). In contrast cells transfected with Alix alone had little effect on cell death and was not significantly different from lipofectamine only controls.

However, in the absence of NMDA/glycine treatment, cells expressing NMDARs+Alix displayed a high level of cell death (mean cell death of  $17.3 \pm 1.0$  %, Figure 3B). This level of cell death was significantly higher than cell only controls (mean cell death= $11.9 \pm 0.7$  %), Alix only cells (mean cell death= $12.4 \pm 0.8$  %) or cells only expressing NMDARs ( $11.6 \pm 0.7$  %) (ANOVA  $p<0.001$ ). This indicates that GluN1/GluN2A/Alix transfection enhanced the basal level of cell death in the absence of NMDA. Therefore, this would suggest that coexpression of Alix is exerting an influence on NMDAR triggered cell death especially at low levels of NMDAR activation or low agonist concentrations.

We next repeated the NMDAR cell death assay in the presence of the competitive NMDAR antagonist, APV to confirm that the effects induced by Alix in the absence of NMDAR activation were directly caused by stimulation of the NMDA receptor (Figure 3C). We found that by adding APV to the medium during NMDA/glycine treatment reduced cell death seen in Figure 3A (Mean cell death GluN1/GluN2A=9.8 ± 1.9 %, Mean cell death GluN1/GluN2A/Alix=9.3 ± 2.8 %) to similar levels seen in the cells only control (Mean cell death=8.3 ± 1.3%). In the presence of APV, the enhanced cell death seen in the absence of NMDA/glycine in cells transfected with GluN1/GluN2A/Alix was abolished (Figure 3D, mean cell death=11.7 ± 4 %). Furthermore, we excluded the influence of the GluN1 or GluN2A expression vectors by repeating the cell death assay with cotransfections of Alix and GluN1 or Alix with GluN2A and found that there was no significant change in cell death compared to the cells only control in the absence or presence of NMDA/glycine (Figure 3E and F). Therefore, the increased levels of cell death seen in cells transfected with NMDAR + Alix (Figure 3B) require the formation of functional NMDARs and NMDAR activation.

The enhanced NMDAR cell death in cells expressing Alix/NMDARs (Figure 3B) suggest that cells expressing NMDAR+Alix exhibit an increased sensitivity to lower concentrations of glutamate/glycine. Basal levels of cell death have been attributed to low levels of amino acids present within the culture media which could stimulate functional NMDARs expressed in GluN1/GluN2A transfected cells [25]. We examined this further by measuring the extent of cell death under a range of NMDA concentrations (0.1 mM, 0.3 mM, 0.7 mM, 1 mM) on cells expressing GluN1/GluN2A NMDARs or GluN1/GluN2A NMDARs +Alix (Figure 4). Higher levels of cell death were observed in the presence of Alix at low concentrations of NMDA (0.1-0.3 mM) compared to cells expressing only GluN1/GluN2A subunits. This further supported our assumption that the expression of Alix is lowering the

NMDA concentration required to trigger maximal levels of cell death in our assay (>20 %) and suggests that the enhanced cell death in the presence of Alix seen in non-treated cells is probably caused by low levels of NMDAR activation. Estimation of the NMDA EC<sub>50</sub>s also revealed a higher NMDA sensitivity in cells expressing Alix (NMDA EC<sub>50</sub>=0.8 ± 0.01 mM for GluN1/GluN2A cells versus NMDA EC<sub>50</sub>=0.10 ± 0.02 mM for GluN1/GluN2A/Alix cells). Therefore, this would imply that Alix is increasing the potency of NMDAR-triggered cell death compared to cells only expressing NMDARs.

We then investigated the regions of Alix which might be responsible for our observations in Figure 3B. The Alix protein contains a number of functional domains and proline-rich amino acid residues within the N-terminal and C-terminal regions of Alix. The N- and C-terminal regions are linked by a stretch of amino acid residues containing two coiled-coil domains [29](Figure 1A). Therefore, to confirm our observations were not specific to the human Alix sequence or influenced by the GFP-tag, we coexpressed wildtype and deletion mutants of mouse Alix (mouse FLAG tagged Alix WT, mouse Alix NT (N-terminal regions covering amino acids residues 1 to 434) and mouse Alix CT (C-terminal regions covering amino acid residues 468 to 869) to determine the effect these variants had on the NMDAR cell death assay (Figure 1A, Figure 5). Cells transfected with wildtype mouse Alix produced a similar pattern as the human Alix when coexpressed with NMDARs (Figure 5A and B). Mouse Alix reduced the toxicity associated with NMDA receptor stimulation when treated with NMDA/glycine (Mean cell death=18.6 ± 1.9 %) compared to GluN1/GluN2A only cells (Mean cell death=23.1 ± 1.1 %), but this difference was not found to be statistically significant. However, we observed enhanced cell death in the absence of NMDA/glycine treatment (Mean cell death=15.6 ± 1.1 %) compared to cells only (Mean cell death=9.3 ± 0.9 %) or GluN1/GluN2A only cells (8.2 ± 0.4 %, ANOVA, p<0.01) (Figure 5B). We examined whether the Alix deletion mutants also showed elevated cell death in the

This article is protected by copyright. All rights reserved.

absence of NMDA/glycine. AlixCT/NMDAR cells displayed an elevated level of cell death compared to NMDAR only cells (Mean cell death= $15.9 \pm 0.3$  % vs NMDAR only mean cell death= $11 \pm 1.1$ %, ANOVA,  $p < 0.05$ , Figure 5C). But this was not seen with AlixNT/NMDAR cells (Mean cell death= $11.3 \pm 0.3$  %, Figure 5D), compared to cells only controls (Mean cell death= $10.6 \pm 0.3$  %, Figure 5D) or cells expressing GluN1/GluN2A subunits only (Mean cell death= $10.3 \pm 0.4$  %, Figure 5D). Therefore, this supports the conclusion that the C terminal domain of the Alix protein is responsible for the enhanced NMDAR cell death seen in the absence of NMDA/glycine described in Figure 3B.

Previous work has shown that the  $Ca^{2+}$ -dependent interaction between Alix and ALG2 is thought to be important for triggering cell death and this interaction involves a proline rich region (residues 802-813) within the C-terminal domain [11]. To examine whether our observations are dependent on the Alix-ALG-2 interaction, we expressed an Alix mutant (mouse deltaPRD) spanning amino acid residues 1-717 [17] (Figure 1A, Figure 5E). In the absence of NMDAR stimulation, we still observed a significantly elevated level of cell death (Mean cell death= $17.5 \pm 0.2$  % vs NMDAR only mean cell death= $10 \pm 0.5$ %, ANOVA,  $p < 0.001$ ) compared to controls similar to that seen in the presence of the AlixCT mutant (Figure 5E). Therefore, other domains within the Alix C-terminal domain are responsible for the enhanced level of cell death under these conditions and imply the involvement of a signalling pathway or interaction that could be independent of ALG-2-Alix binding.

## Discussion

This is the first report describing the potential functional interaction of Alix and glutamate receptors. Our results from heterologous expression of recombinant Alix and NMDARs suggest that Alix could influence the downstream effects of NMDAR activation

and highlight a potential role of the C-terminal region of the Alix protein in increasing the sensitivity of NMDARs to trigger cell death. Our partial dose-response curves suggest that the coexpression of Alix decreased the NMDA  $EC_{50}$  for inducing cell death by 7-fold compared to NMDARs expressed alone. However, the NMDA  $EC_{50}$  values measured in the cell death assay differ quite considerably compared to those measured in other systems where recombinant NMDA receptor function has been recorded by oocyte electrophysiology (NMDA  $EC_{50} = 47 \mu\text{M}$ ) [30]. There are a number of reasons for this discrepancy and this has probably been influenced by the transfection efficiency of both GluN1 and GluN2A subunits within the same cell, the ability to detect changes in cell death over prolonged periods of time and the influence of multiple second messenger pathways needed before cell death is detected. Nevertheless there is common agreement that  $EC_{50}$  values cannot be easily compared across different tissue systems/assay measurements and their interpretation has to be used appropriately [31].

Our data does suggest that some regions within the Alix C-terminal domain excluding the proline-rich region directly/indirectly enhance cell death as long as there is sufficient NMDAR activation (and presumably  $\text{Ca}^{2+}$  influx). The role of a number of domains linked with cell death processes have been identified within the N-terminal domain (Bro1 interaction with CHMP4) and the proline-rich region within the C-terminal domain (endophilins and ALG-2) [11,32]. Furthermore, the route of  $\text{Ca}^{2+}$  entry also has important implications for cell death [2] and dissecting the precise necrotic or apoptotic mechanisms underlying NMDAR cell death can be complex and depend on the intensity/duration of glutamate stimulation [33,34]. In addition, we cannot exclude the possibility that Alix might influence the kinetics of NMDAR inward currents upstream of any intracellular signalling cascades following receptor activation. Therefore, any upregulation of these signalling cascades, possibly by slowing the deactivation of NMDAR currents (and thus increase  $\text{Ca}^{2+}$  influx) could explain

This article is protected by copyright. All rights reserved.

the leftward shift of the dose-response curve in the presence of Alix. However, is there evidence for Alix expressed at synaptic sites? Although we have not demonstrated a direct interaction with NMDARs, there are several lines of evidence supporting the potential for close localisation. Firstly, Alix is found within the postsynaptic density [18,19] and secondly Alix is known to interact with dopamine receptors [14] and can alter pharmacological properties. Furthermore, there are known direct protein interactions between dopamine receptors and NMDARs [20,21] and both receptors can form dynamic cell surface clusters in neurones near glutamatergic synapses [35] and even if Alix does not interact directly, there would be potential opportunities for Alix to influence signalling downstream of NMDARs.

It is unclear why Alix was able to reduce cell death in the presence of NMDA/glycine when coexpressed with NMDARs (Figure 3A). Our observations suggest that this requires NMDAR expression and NMDAR activation (Figure 3C-F). Previous work has shown that overexpression of the Alix C-terminal domain can inhibit apoptotic processes and reduce neuronal cell death by blocking Alix interaction with endogenous ALG-2 [7] [11] [10,32].

The interaction between Alix and ALG-2 occurs through its C-terminal proline-rich region and is known to be  $Ca^{2+}$  dependent [7] [6]. ALG-2 is endogenously expressed in HEK293 cells [7] and the protein levels of Alix to ALG-2 could have important implications for cell death. However, from our data expression of the Alix mutant lacking the proline-rich region in the C-terminal still displayed high levels of NMDAR-triggered cell death in the absence of

NMDA/glycine.

There is strong evidence that endogenous Alix is highly expressed in neurones following transient and chronic neuronal insults. Hemming et al., 2004 [9] found that Alix expression was increased in areas of high c-fos expression and in dying neuronal cell bodies after kainate. This article is protected by copyright. All rights reserved.

induced neurodegeneration. Increased Alix expression persisted 24 hours after kainate injection in the piriform cortex and it has been postulated that Alix may play an early role in the cell death mechanism. To support this, Blum et al., 2004 [36] also found Alix upregulation in neuronal cell bodies within the cortex and lateral striatum following chronic neurodegeneration by 3-nitropropionic acid. However, it is not completely clear whether Alix is a trigger or an early marker for neurodegenerative processes. Alix is known to be a component of the synaptic ESCRT-III complex associated with the spinoskeleton and loss of Alix has been shown to disrupt normal cytoskeletal organization within the cell [37]. Hence Alix may play an important role in supporting the structure of the PSD within dendritic spines [19]. The importance of maintaining a normal ESCRT-III complex is highlighted by C-terminal truncations in one of the core components of the ESCRT-III complex, Chmp2b that have been linked to familial frontotemporal dementia [38].

In summary, we have identified a potential role for Alix with NMDAR activation and given the proximity of both of these proteins within the postsynaptic density could indicate an additional route by which NMDAR downstream signalling may be modified during neuronal cell death. Nevertheless, further work is required to fully elucidate the potential contribution of Alix in these downstream signalling cascades.

**Acknowledgments:** We are grateful for the gift of Alix cDNA plasmids from Remy Sadoul and NMDAR cDNA plasmids from Stephanie Schorge and Pavlos Alifragis for help with the confocal microscopy. S.S. was funded by a South West Academic Network (SWAN) PhD

This article is protected by copyright. All rights reserved.

studentship.

### Author Contributions:

P.E.C., J.N. and S.S. conceived and designed the experiments; S.S. performed the experiments; S.S. and P.E.C. analyzed the data; S.S. J.N. and P.E.C. wrote the paper.

### References

- [1] Choi, D.W. (1990). Possible mechanisms limiting N-methyl-D-aspartate receptor overactivation and the therapeutic efficacy of N-methyl-D-aspartate antagonists. *Stroke* 21, III20-2.
- [2] Szydłowska, K. and Tymianski, M. (2010). Calcium, ischemia and excitotoxicity. *Cell Calcium* 47, 122-9.
- [3] Hardingham, G.E. and Bading, H. (2010). Synaptic versus extrasynaptic NMDA receptor signalling: implications for neurodegenerative disorders. *Nat Rev Neurosci* 11, 682-96.
- [4] Wyllie, D.J., Livesey, M.R. and Hardingham, G.E. (2013). Influence of GluN2 subunit identity on NMDA receptor function. *Neuropharmacology* 74, 4-17.
- [5] Hansen, K.B., Yi, F., Perszyk, R.E., Furukawa, H., Wollmuth, L.P., Gibb, A.J. and Traynelis, S.F. (2018). Structure, function, and allosteric modulation of NMDA receptors. *J Gen Physiol* 150, 1081-1105.
- [6] Missotten, M., Nichols, A., Rieger, K. and Sadoul, R. (1999). Alix, a novel mouse protein undergoing calcium-dependent interaction with the apoptosis-linked-gene 2 (ALG-2) protein. *Cell Death Differ* 6, 124-9.
- [7] Vito, P., Pellegrini, L., Guiet, C. and D'Adamio, L. (1999). Cloning of AIP1, a novel protein that associates with the apoptosis-linked gene ALG-2 in a Ca<sup>2+</sup>-dependent reaction. *J Biol Chem* 274, 1533-40.
- [8] Katoh, K., Shibata, H., Suzuki, H., Nara, A., Ishidoh, K., Kominami, E., Yoshimori, T. and Maki, M. (2003). The ALG-2-interacting protein Alix associates with CHMP4b, a human homologue of yeast Snf7 that is involved in multivesicular body sorting. *J Biol Chem* 278, 39104-13.
- [9] Hemming, F.J., Fraboulet, S., Blot, B. and Sadoul, R. (2004). Early increase of apoptosis-linked gene-2 interacting protein X in areas of kainate-induced neurodegeneration. *Neuroscience* 123, 887-95.
- [10] Strappazzon, F., Torch, S., Chatellard-Causse, C., Petiot, A., Thibert, C., Blot, B., Verna, J.M. and Sadoul, R. (2010). Alix is involved in caspase 9 activation during calcium-induced apoptosis. *Biochem Biophys Res Commun* 397, 64-9.
- [11] Trioulier, Y., Torch, S., Blot, B., Cristina, N., Chatellard-Causse, C., Verna, J.M. and Sadoul, R. (2004). Alix, a protein regulating endosomal trafficking, is involved in neuronal death. *J Biol Chem* 279, 2046-52.
- [12] Mercier, V. et al. (2016). ALG-2 interacting protein-X (Alix) is essential for clathrin-independent endocytosis and signaling. *Sci Rep* 6, 26986.

- [13] Laporte, M.H. et al. (2017). Alix is required during development for normal growth of the mouse brain. *Sci Rep* 7, 44767.
- [14] Zhan, L., Liu, B., Jose-Lafuente, M., Chibalina, M.V., Grierson, A., Maclean, A. and Nasir, J. (2008). ALG-2 interacting protein AIP1: a novel link between D1 and D3 signalling. *Eur J Neurosci* 27, 1626-33.
- [15] Mahul-Mellier, A.L. et al. (2009). Alix and ALG-2 make a link between endosomes and neuronal death. *Biochem Soc Trans* 37, 200-3.
- [16] Sadoul, R., Laporte, M.H., Chassefeyre, R., Chi, K.I., Goldberg, Y., Chatellard, C., Hemming, F.J. and Fraboulet, S. (2018). The role of ESCRT during development and functioning of the nervous system. *Semin Cell Dev Biol* 74, 40-49.
- [17] Chatellard-Causse, C., Blot, B., Cristina, N., Torch, S., Missotten, M. and Sadoul, R. (2002). Alix (ALG-2-interacting protein X), a protein involved in apoptosis, binds to endophilins and induces cytoplasmic vacuolization. *J Biol Chem* 277, 29108-15.
- [18] Bayes, A., van de Lagemaat, L.N., Collins, M.O., Croning, M.D., Whittle, I.R., Choudhary, J.S. and Grant, S.G. (2011). Characterization of the proteome, diseases and evolution of the human postsynaptic density. *Nat Neurosci* 14, 19-21.
- [19] Chassefeyre, R. et al. (2015). Regulation of postsynaptic function by the dementiarelated ESCRT-III subunit CHMP2B. *J Neurosci* 35, 3155-73.
- [20] Lee, F.J. et al. (2002). Dual regulation of NMDA receptor functions by direct proteinprotein interactions with the dopamine D1 receptor. *Cell* 111, 219-30.
- [21] Liu, X.Y. et al. (2006). Modulation of D2R-NR2B interactions in response to cocaine. *Neuron* 52, 897-909.
- [22] Devor, A. et al. (2017). Genetic evidence for role of integration of fast and slow neurotransmission in schizophrenia. *Mol Psychiatry* 22, 792-801.
- [23] Schorge, S. and Colquhoun, D. (2003). Studies of NMDA receptor function and stoichiometry with truncated and tandem subunits. *J Neurosci* 23, 1151-8.
- [24] Hajos, F. (1975). An improved method for the preparation of synaptosomal fractions in high purity. *Brain Res* 93, 485-9.
- [25] Wagey, R., Hu, J., Pelech, S.L., Raymond, L.A. and Krieger, C. (2001). Modulation of NMDA-mediated excitotoxicity by protein kinase C. *J Neurochem* 78, 715-26.
- [26] Boeck, C.R., Bronzatto, M.J., Souza, D.G., Sarkis, J.J. and Vendite, D. (2000). The modulation of ecto-nucleotidase activities by glutamate in cultured cerebellar granule cells. *Neuroreport* 11, 709-12.
- [27] Hogins, J., Crawford, D.C., Zorumski, C.F. and Mennerick, S. (2011). Excitotoxicity triggered by Neurobasal culture medium. *PLoS One* 6, e25633.
- [28] Dores, M.R., Chen, B., Lin, H., Soh, U.J., Paing, M.M., Montagne, W.A., Meerloo, T. and Trejo, J. (2012). ALIX binds a YPX(3)L motif of the GPCR PAR1 and mediates ubiquitin-independent ESCRT-III/MVB sorting. *J Cell Biol* 197, 407-19.
- [29] Odorizzi, G. (2006). The multiple personalities of Alix. *J Cell Sci* 119, 3025-32.
- [30] Chen, P.E. et al. (2005). Structural features of the glutamate binding site in recombinant NR1/NR2A N-methyl-D-aspartate receptors determined by site-directed mutagenesis and molecular modeling. *Mol Pharmacol* 67, 1470-84.
- [31] Colquhoun, D. (1998). Binding, gating, affinity and efficacy: the interpretation of structure-activity relationships for agonists and of the effects of mutating receptors. *Br J Pharmacol* 125, 924-47.
- [32] Mahul-Mellier, A.L., Hemming, F.J., Blot, B., Fraboulet, S. and Sadoul, R. (2006). Alix, making a link between apoptosis-linked gene-2, the endosomal sorting complexes required for transport, and neuronal death in vivo. *J Neurosci* 26, 542-9.

- [33] Bonfoco, E., Krainc, D., Ankarcrona, M., Nicotera, P. and Lipton, S.A. (1995). Apoptosis and necrosis: two distinct events induced, respectively, by mild and intense insults with N-methyl-D-aspartate or nitric oxide/superoxide in cortical cell cultures. *Proc Natl Acad Sci U S A* 92, 7162-6.
- [34] Ankarcrona, M., Dypbukt, J.M., Bonfoco, E., Zhivotovsky, B., Orrenius, S., Lipton, S.A. and Nicotera, P. (1995). Glutamate-induced neuronal death: a succession of necrosis or apoptosis depending on mitochondrial function. *Neuron* 15, 961-73.
- [35] Ladepeche, L. et al. (2013). Single-molecule imaging of the functional crosstalk between surface NMDA and dopamine D1 receptors. *Proc Natl Acad Sci U S A* 110, 18005-10.
- [36] Blum, D., Hemming, F.J., Galas, M.C., Torch, S., Cuvelier, L., Schiffmann, S.N. and Sadoul, R. (2004). Increased Alix (apoptosis-linked gene-2 interacting protein X) immunoreactivity in the degenerating striatum of rats chronically treated by 3nitropropionic acid. *Neurosci Lett* 368, 309-13.
- [37] Cabezas, A., Bache, K.G., Brech, A. and Stenmark, H. (2005). Alix regulates cortical actin and the spatial distribution of endosomes. *J Cell Sci* 118, 2625-35.
- [38] Isaacs, A.M., Johannsen, P., Holm, I., Nielsen, J.E. and consortium, F.R. (2011). Frontotemporal dementia caused by CHMP2B mutations. *Curr Alzheimer Res* 8, 24651.

## Figure Legends

Figure 1- Expression and intracellular distribution of transiently transfected GFP-tagged Alix in HEK293 cells. A. Schematic diagram of human and mouse Alix cDNAs expressed in HEK 293 cells. Green region indicates location of GFP tag, red region indicates the predicted Bro1 sequence and the grey region indicates the proline rich domain. B. Western blotting confirmed expression of recombinant GFP-hAlix at 123 kDa (top) and GluN1 (bottom) at 108 kDa in transfected HEK293 cells (arrowhead) which was absent in cell only lysates. Intracellular distribution of Alix is shown in C-E (cells expressing Alix alone) and F-J (cells expressing Alix with NMDARs). Green fluorescence denotes Alix expression (C and F))

while blue corresponds to Hoechst 33342 stained nuclei (D and G). The merged image of panels C-D and F-G is shown in E and H respectively. I-J. Cells expressing NMDARs were also stained for GluN1 expression and the merged image with Alix expression (F) is shown in I. Scale Bar: 10  $\mu$ m. Anti-GluN1 mouse antibody (BD Biosciences, 1:1000 dilution), Alexa Fluor 488 Goat anti-mouse (Invitrogen, 1:1000 dilution).

Figure 2- Expression of endogenous Alix from rat brain synaptosomal fractions and intracellular distribution in rat primary cortical neurones. A. Western blot showing endogenous expression of GluN1 (108 kDa) and Alix (96 kDa) in different subcellular fractions from adult rat brain. Syn, synaptosomal, LM, light membrane, Myl, myelin, Mito, mitochondrial and Ad, adult rat brain homogenate. B-M. Immunocytochemistry from rat primary cortical neurones (DIV14). Endogenous Alix expression is shown (B, green, F and J, red) while blue corresponds to Hoechst 33342 stained nuclei (C, G, K) and red F-actin visualised with TRITC-conjugated rhodamine-phalloidin (D), rabbit anti-PSD-95 (H) and mouse anti-EEA1 (L). The merged image of panels B-D is shown in E, F-H in I and J-L in M. Scale Bar: 10  $\mu$ m. Anti-Alix mouse antibody (Abcam, 1:100 dilution), anti-PSD95 rabbit antibody (Abcam, 1:500 dilution), anti-EEA1 mouse antibody (BD Biosciences, 1:1000 dilution), Alexa Fluor 488 goat anti-mouse and donkey anti-rabbit (Invitrogen, 1:1000 dilution).

Figure 3- Cotransfection of GFP tagged human Alix + GluN1/GluN2A NMDARs in HEK293 cells influences NMDAR-triggered cell death. A. Mean percentage cell death measured by trypan blue exclusion following application of 1 mM NMDA/50  $\mu$ M glycine, n=7-12. \*\* p<0.01 NMDAR only vs Alix+NMDAR B. Mean percentage cell death in PSS only exposure, n=7-14. \*\*\* p<0.001 NMDAR only vs Alix+NMDAR C. Mean cell death in the presence of 1 mM NMDA/50  $\mu$ M glycine exposure + 100  $\mu$ M APV, n=3. D. Mean cell death

following PSS only exposure + 100  $\mu$ M APV, n=3. E. Mean cell death following separate cDNA plasmid transfection + 1 mM NMDA/50  $\mu$ M glycine exposure, n=3. F. Mean cell death following separate cDNA plasmid transfection + PSS exposure, n=3.

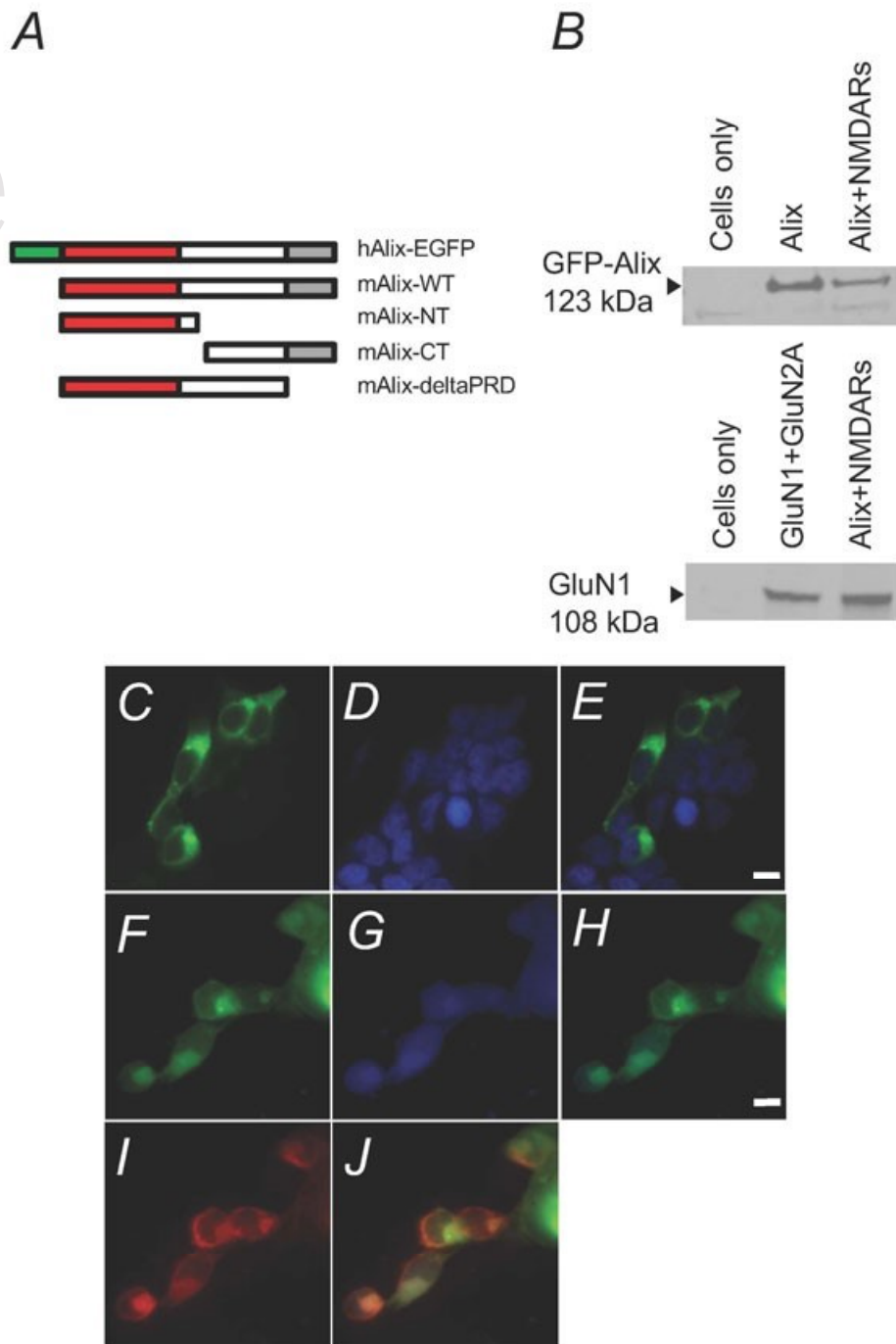
Figure 4- Partial NMDA dose-response curves of NMDAR-triggered cell death in GluN1/GluN2A only and GluN1/GluN2A + Alix expressing cells. In the presence of Alix (grey filled circles), low concentrations (0.1-0.3 mM) of NMDA trigger far higher levels of cell death compared to cells expressing GluN1/GluN2A only (black filled squares), n=3. Both dose-response curves were fit with the Hill equation predicting NMDA EC<sub>50</sub> = 0.8  $\pm$  0.01 mM (GluN1/GluN2A) and NMDA EC<sub>50</sub> = 0.10  $\pm$  0.02 mM (GluN1/GluN2A+Alix). Dashed lines represent curves extrapolated to the basal levels of cell death.

Figure 5. Overexpression of wildtype mouse Alix and Alix deletion mutants influence NMDA-triggered cell death.

Mean cell death was measured using trypan blue exclusion in the presence (A) and absence (B) of 1 mM NMDA/ 50  $\mu$ M glycine. (A,B) Cotransfection of Flag tagged mouse Alix + GluN1/GluN2A NMDARs influences NMDAR-triggered cell death. A. 1mM NMDA/50  $\mu$ M glycine exposure. B. PSS only exposure reveals enhanced cell death in the presence of Alix+NMDARs \*\* p<0.01 NMDAR only vs mouse Alix+NMDAR. C. Deletion mutants of mouse Alix displayed elevated cell death with AlixCT \* p<0.05 NMDAR only vs AlixCT+NMDAR. D. This was not seen with AlixNT in the presence of PSS. E. Removal of the PRD domain did not prevent NMDAR-triggered cell death in the presence of PSS. \*\*\* p<0.001 NMDAR only cells vs mouse Alix $\Delta$ PRD +NMDAR cells. All experiments n=3.

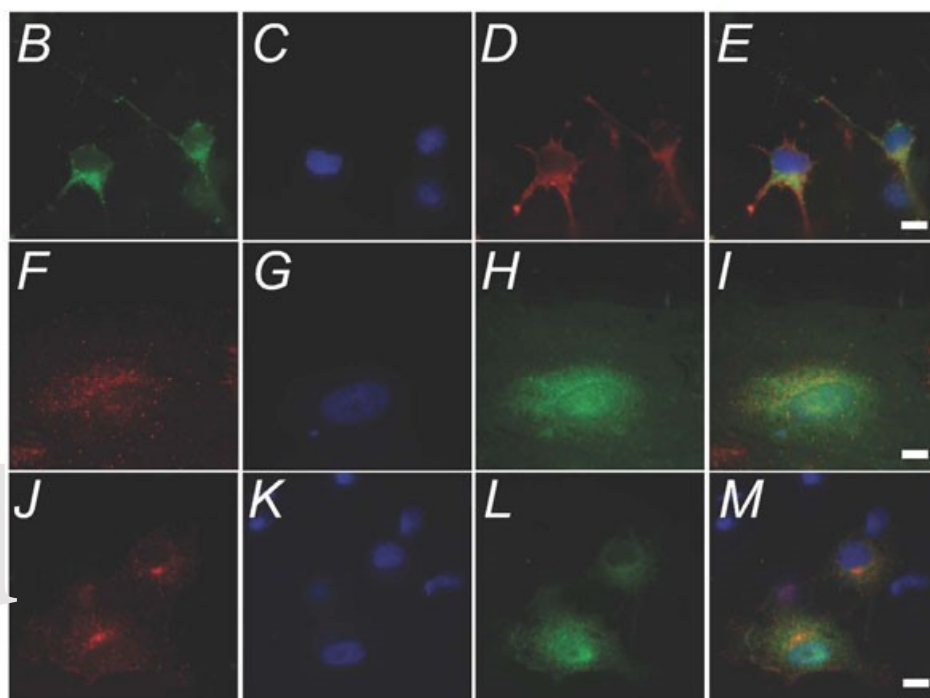
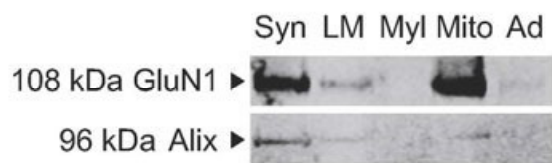


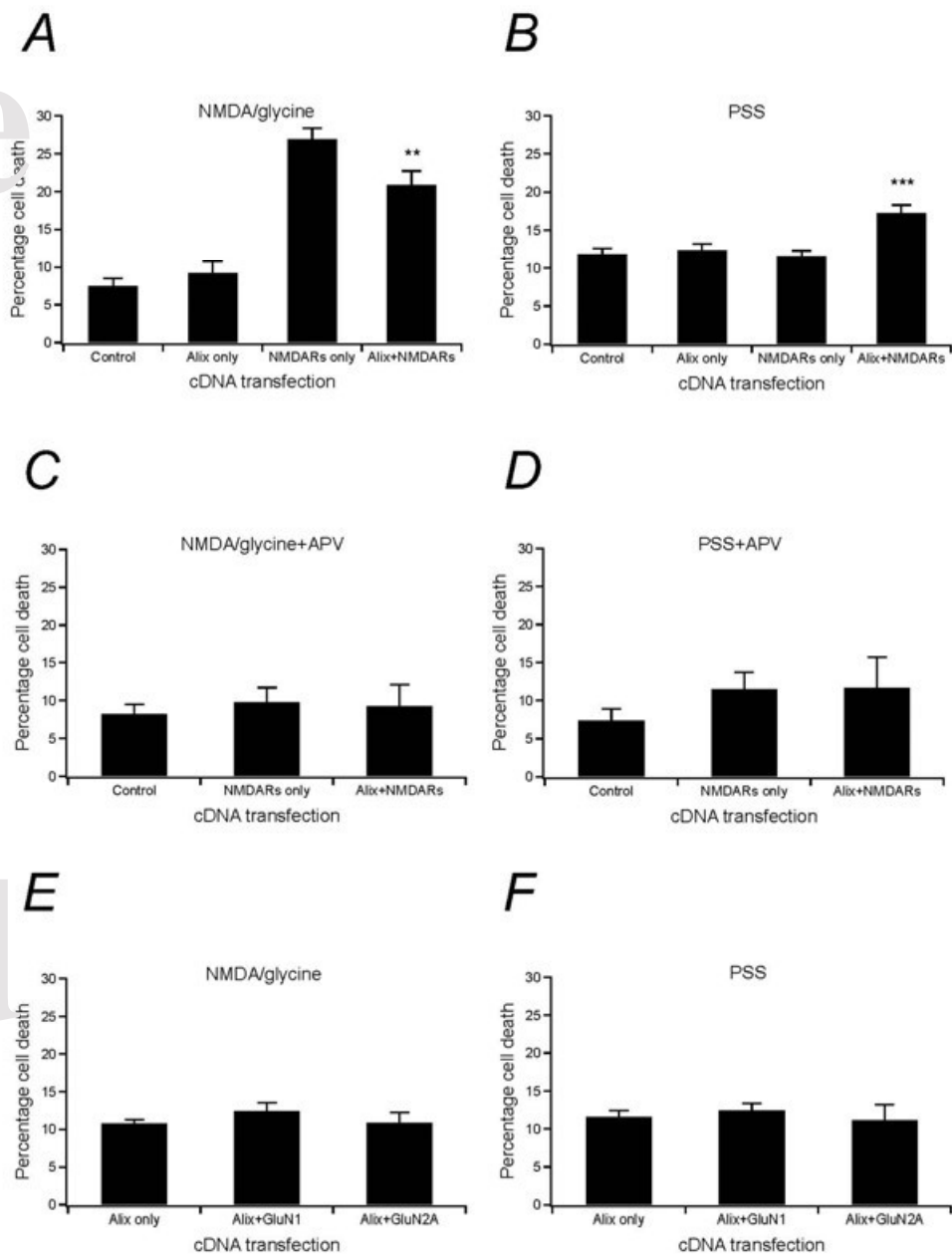
Article



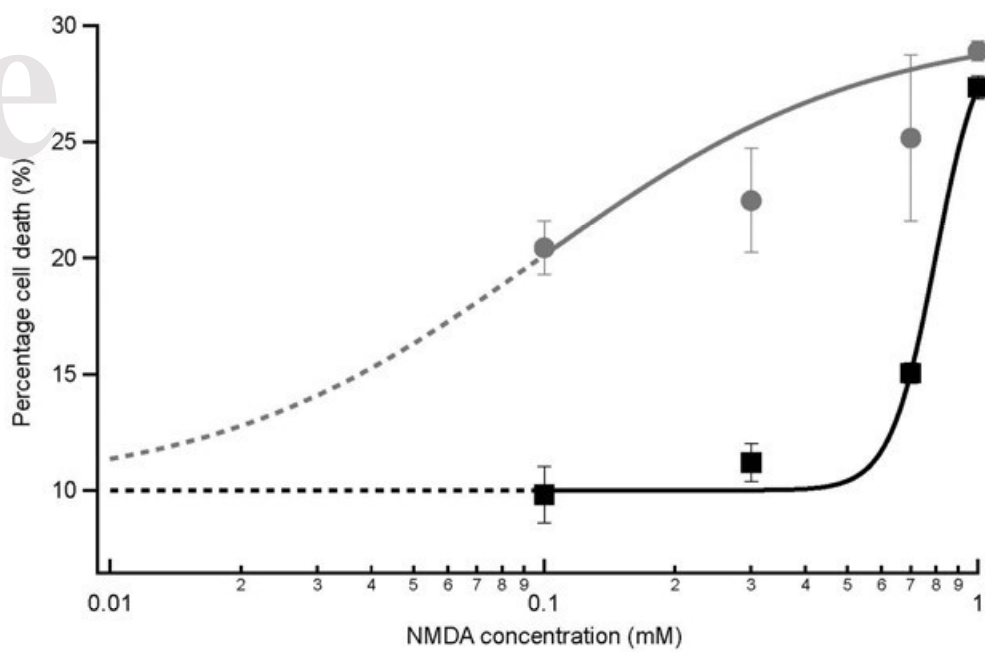
oted

A



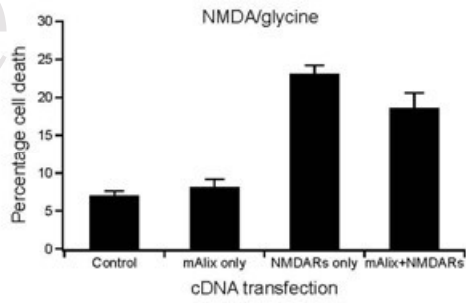


Article

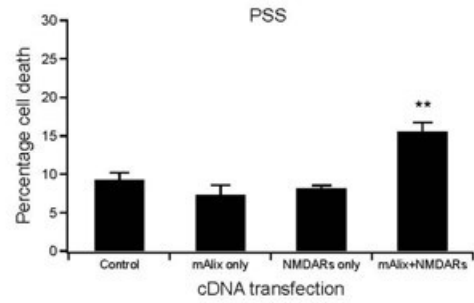


oted

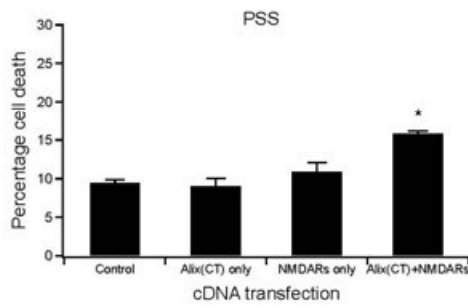
**A**



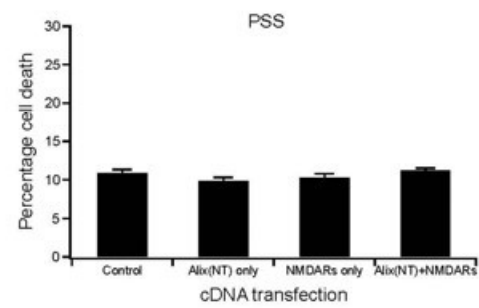
**B**



**C**



**D**



**E**

